Rare Gases on Noble-Metal Surfaces: An Angle-Resolved Photoemission Study with High Energy Resolution†

F. Forster and S. Hüfner

Universität des Saarlandes, FR 7.2 Experimentalphysik, D-66041 Saarbrücken, Germany

F. Reinert*

Universität Würzburg, Experimentelle Physik II, D-97074 Würzburg, Germany

Received: February 20, 2004; In Final Form: June 15, 2004

In this paper, we present a systematic angle-resolved photoemission (ARUPS) study on prototypical adsorbate systems consisting of a rare-gas monolayer (Ar, Kr, Xe) on a noble-metal (111) surface (Cu, Ag, Au). Although the coupling between substrate and physisorbed overlayer is weak, there is a significant influence on the Shockley-type surface state that is still observable on the well-ordered monolayer systems. The results show that there is an immediate correspondence between the surface-state binding energy and the nobleness of the rare-gas adsorbates, reflecting the short-range repulsive forces between adsorbate and substrate. In the case of Au(111), one can observe an increase of the spin−orbit splitting of the Shockley state with decreasing nobleness. In addition, we discuss the influence of the $\sqrt{3} \times \sqrt{3}R30°$ Xe superlattice on the surface electronic structure of Cu(111).

1. Introduction

Shockley states are particular electronic states that are confined to the surface region of a solid.[1] Since their first experimental observation by photoemission spectroscopy (PES) on Cu(111) about 30 years ago,[2] they have been investigated experimentally on many different metal surfaces. Shockley states form a quasi-two-dimensional, nearly free electron system of sp-derived states within the band gap of the projected bulk states close to the Fermi level.[3] These properties make Shockley states in general suitable for investigation by surface-sensitive experimental techniques such as angle-resolved photoemission spectroscopy (ARUPS; see, e.g., refs 4−6) or scanning tunneling microscopy (STM; see, e.g., refs 7−9). In addition, the Shockley-type surface states are theoretically very well understood and most physical properties can be calculated precisely, e.g., their electronic band dispersion or the influence of many-body interaction on the intrinsic lifetime width.[10−12] In particular, Shockley states on the (111) faces of noble metals have been thoroughly investigated by experimental and theoretical techniques.

In contrast to bulk states of solids, the electrons of surface states are localized to the first few atomic layers at the surface. Therefore, they strongly influence the interaction between the surface and its environment and thereby contribute to the chemistry of surfaces, such as adsorption processes, equilibrium surface structures, or catalytic reactions.[13] At the same time, the spectroscopic investigation of surface states offers a sensitive probe for surface modifications or, more fundamentally, for adsorbate−substrate interactions.

The simplest model system for the investigation of the influence of surface modifications on the surface electronic structure is a rare-gas monolayer on a noble-metal substrate. At low temperatures, the gas atoms are physisorbed by dispersion or van der Waals forces with typical binding energies of only 50−500 meV per atom.[14] Consequently, the desorption temperatures are in the range of a few tens of Kelvin. The van der Waals forces interact with the short-range repulsive force between the substrate and the closed-shell configuration of the rare-gas atoms, usually called Pauli repulsion.[15] The repulsive interaction can be related to shifts in the binding energy of the Bloch electrons,[16,17] which is generally accessible by photoemission spectroscopy. Because the interaction between the rare-gas atoms and the metal substrate is weak, the Shockley states can still be observed when the substrate is covered by a well-ordered monolayer. However, the surface electronic structure is influenced significantly by the presence of the rare-gas adsorbate, e.g., the position of the Shockley-state band minimum can be shifted by several 10 meV in comparison to its position on the clean surface. For adsorbate systems with a stronger coupling between adsorbate and substrate the Shockley state can shift above the Fermi level or disappear completely, e.g. for Xe on Ag(111) (see below) or PTCDA on Cu(111).[18] In fact, the Shockley state is always a property of the whole system consisting of the substrate and the adsorbed layer. Despite the simplicity of the model systems discussed in this paper, several fundamental questions have not been answered satisfactorily, in particular, the question of the nature of the adsorbate−surface bond.

Here, we present a systematic photoemission study of the Shockley states of various monolayer systems of the rare gases Ar, Kr, and Xe on the substrates Cu(111), Ag(111), and Au(111). By use of high-resolution angle-resolved photoemission (ARUPS), we determined the influence of the adsorbate on the surface-state band dispersion, i.e., the electronic binding energies and the effective band masses, and in the case of Au(111), the change of the characteristic spin−orbit splitting.

2. Experimental Setup and Sample Preparation

The experiments presented here were performed with a high-resolution photoelectron spectrometer equipped with a monochromatized VUV source (GAMMADATA) and a SCIENTA SES-200 photoelectron analyzer. The angular resolution of the analyzer in the angular mode is $\Delta\theta = 0.3°$; the energy resolution, consisting of broadenings from both the light source (He−I) and the analyzer, amounts to $\Delta E \approx 3$ meV.[19−21] The

† Part of the special issue "Gerhard Ertl Festschrift".

* Corresponding author. Fax: +49 931 888 5158. E-mail: reinert@physik.uni-wuerzburg.de.

10.1021/jp049215b CCC: $27.50
Published on Web 07/28/2004

base pressure was 4×10^{-11} mbar, increasing to 9×10^{-10} mbar during the measurements due to He leakage from the discharge lamp. The surfaces of the single-crystal substrates (MaTecK) were cleaned by the standard sputtering−annealing cycles.[22,23]

The adsorbates were applied slowly at a partial pressure of $\sim 3 \times 10^{-8}$ mbar at low temperatures in situ at the measurement position, while the coverage was monitored in real time by a comparison of the photoemission intensities of the surface state of covered and uncovered areas.[24,25] The individual preparation temperature of each system must be high enough to provide sufficient mobility of the adsorbates to form well-ordered films, but still below the desorption temperature of the first monolayer. The values are given in the respective figure captions. In addition, we checked the surface quality of the substrates and the coverage procedure by low-energy electron diffraction (LEED) with the sample holder mounted on a closed-cycle refrigerator in the preparation chamber.

Using the highly efficient parallel detection mode of the analyzer, one data set, i.e., the photoemission intensity $I(E_B,k_{||})$ of the complete occupied part of a surface-state parabola, could be measured within ~8 min. From such an intensity map (see Figures 1−3), one can extract the energy distribution curves (EDC) and momentum distribution curves (MDC) by taking the intensity vs binding energy, E_B, at constant parallel momentum $k_{||}$ or the intensity vs $k_{||}$ at constant E_B, respectively. The Fermi surface map (FSM) for Xe on Cu(111) given in Figure 6 was obtained by subsequent measurements of MDCs at E_F for different tilt angles, giving the intensity distribution $I(E_F,\mathbf{k}_{||})$, with $\boldsymbol{k}_{||} = (k_x, k_y)$ and the two orthogonal in-plane directions k_x and k_y (for details, see refs 22, 23, and 25).

3. Results

3.1. Clean (111) Surfaces: A Brief Summary. The photoemission experiments on the Shockley states in the *L* gap of the (111) faces of Cu, Ag, and Au have been discussed in detail in ref 23. Therefore, we give only a brief summary of the results here.

The Shockley states of all three investigated surfaces appear centered at the $\bar{\Gamma}$ point of the surface Brillouin zone (SBZ), i.e., with the binding energy maximum at normal emission, and follow a nearly perfect parabolic dispersion with the effective masses and band minima given in Table 1. From normal emission, the states disperse toward the Fermi level, forming a cylindrical Fermi surface with radius k_F within the projected band gap (*L* gap) of the bulk states. In the case of the Shockley state on Au(111), there is a characteristic splitting of the parabola, which is caused by spin−orbit coupling (SOC) in combination with the broken inversion symmetry at the surface.[22,26] In the photoemission data, there appear two parabolas with identical curvature and maximum binding energy, but shifted away from the $\bar{\Gamma}$ point by $\Delta k_{||}/2$, leading to two different Fermi vectors k_F^1 and k_F^2 with $k_F^1 - k_F^2 = \Delta k_{||}$. The energy splitting is zero at $|\mathbf{k}_{||}| = 0$ and increases linearly with increasing $k_{||}$. For further discussions of this SOC split surface state, see refs 27−30.

Subtle deviations from the parabolic dispersion of the bands and details of the photoemission line shapes, caused by many-body effects, are discussed elsewhere[11,12,19,31−33] and can be neglected in the present context.

3.2. Rare Gases on Cu(111). The rare-gas monolayers were prepared on a clean Cu(111) surface as described above. In the case of Ar and Kr, the rare-gas atoms form an incommensurate structure with a nearest-neighbor distance slightly expanded compared to 1×1. In contrast, Xe forms a commensurate $\sqrt{3} \times \sqrt{3}R30°$ superlattice on Cu(111), with the Xe atoms located at on-top sites[35] (see below). This is the only commensurate superstructure among the adsorbate systems investigated here.

TABLE 1: Summary of the Photoemission Results for the Maximum Binding Energy E_B^0, the Effective Band Mass m^*/m_e, and the Resulting Fermi Vector k_F of the Shockley States for Different Adsorbate−Substrate Combinations[a]

	Cu(111)	Ag(111)	Au(111)
		clean	
E_B^0 (meV)	434 ± 2	62 ± 3	479 ± 2
m^*/m_e	0.43 ± 0.01	0.42 ± 0.03	0.26 ± 0.01
k_F (Å^{-1})	0.222 ± 0.001	0.082 ± 0.001	$0.169/0.193 \pm 0.001$[b]
		Ar	
E_B^0 (meV)	376 ± 3	-1 ± 3	422 ± 3
m^*/m_e	0.46 ± 0.03	0.46 ± 0.04	0.26 ± 0.03
k_F (Å^{-1})	0.213 ± 0.003	−	$0.158/0.184 \pm 0.001$[b]
		Kr	
E_B^0 (meV)	358 ± 2	-8 ± 2	400 ± 3
m^*/m_e	0.44 ± 0.02	0.44 ± 0.04	0.27 ± 0.02
k_F (Å^{-1})	0.204 ± 0.002	−	$0.152/0.182 \pm 0.001$[b]
		Xe	
E_B^0 (meV)	291 ± 2	$(-52 \pm 2$[c]$)$	340 ± 2
m^*/m_e	0.44 ± 0.02	$(0.42 \pm 0.06$[c]$)$	0.28 ± 0.02
k_F (Å^{-1})	0.183 ± 0.002	−	$0.140/0.173 \pm 0.001$[b]

[a] Temperatures of the measurements on the monolayer systems are given in the figure captions of Figures 1−3; the reference data on the clean surfaces were measured at $T = 30$ K. [b] Spin−orbit splitting. [c] Values from STM; see ref 34.

The influence of the rare-gas monolayer on the surface-state dispersion along $\bar{\Gamma}-\bar{K}$ is shown in Figure 1. The grayscale plot in the upper row represents the photoemission intensity *I* vs the binding energy E_B (vertical axis) and the parallel momentum $k_{||}$ (momentum along $\bar{\Gamma}-\bar{K}$, horizontal axis); as a reference, the dispersion of the clean surface is indicated as a dashed line. The lower row displays the result of a least-squares fit of the peak dispersion by a parabola $E_B = E_B^0 - \hbar^2 k_{||}^2/2m^*$, giving the effective mass m^* and the maximum binding energy E_B^0 at normal emission. The peak positions have either been extracted from the MDCs (close to the Fermi level) or from the EDCs (at high binding energies), depending on the cut from which the position can be determined more precisely. Obviously, the surface state of the covered surfaces is shifted to lower binding energies (toward the Fermi level), whereas the curvature, i.e., the effective mass m^*/m_e, remains constant within the experimental errors (see Table 1). The relative shift increases from left to right. Thus, it is the smallest for Ar (~58 meV) and the largest for Xe (~143 meV).

In contrast to the photoemission data on the clean surface, the projected band gap could not be resolved in these experiments, presumably because of the increased impurity scattering on defects in the adsorbate layer and—in the case of the incommensurate Ar and Kr system—because of the increased background intensity due to the back-folded bulk states.

3.3. Rare Gases on Ag(111). In principle, the same dependence of the surface state on the rare-gas coverage can be observed for the Ag(111) substrate. The main difference is that the band minimum for clean Ag(111) appears at a binding energy of only ~62 meV. Therefore, the interaction with the rare gas shifts the surface state close to or even above the Fermi level. Above the Fermi level, the photoemission intensity decreases steeply, and the spectral information is suppressed by the Fermi distribution. However, at finite temperatures, the information about the electronic states above E_F can partly be restored by the application of a normalization method introduced by Thomas Greber et al. on Ni(111), provided that the energy

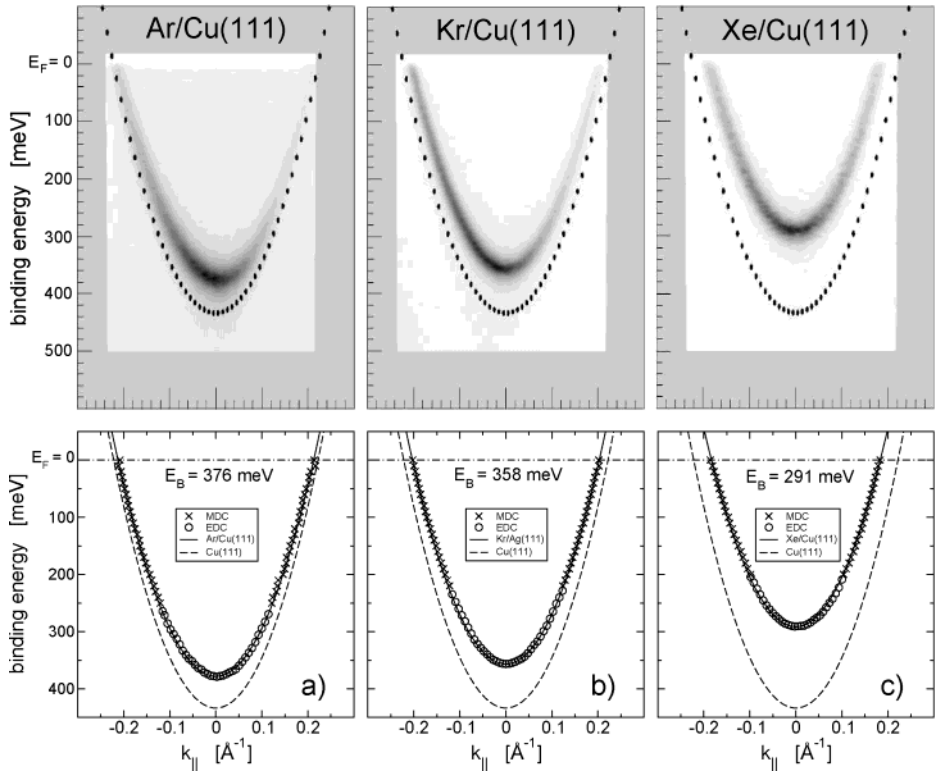

Figure 1. Photoemission data on the Cu(111) surface covered with 1 ML of different rare gases. The grayscale plot in the upper panel gives the photoemission intensity vs binding energy and parallel momentum along the $\bar{\Gamma}-\bar{K}$ direction (dark is high intensity). The dispersion of the clean Cu(111) surface is indicated as a dashed line. The temperatures during preparation and measurement were kept constant at $T = 25$, 35, and 50 K for Ar, Kr, and Xe, respectively. Lower panel: Analysis of the dispersions by a parabolic least-squares fit.

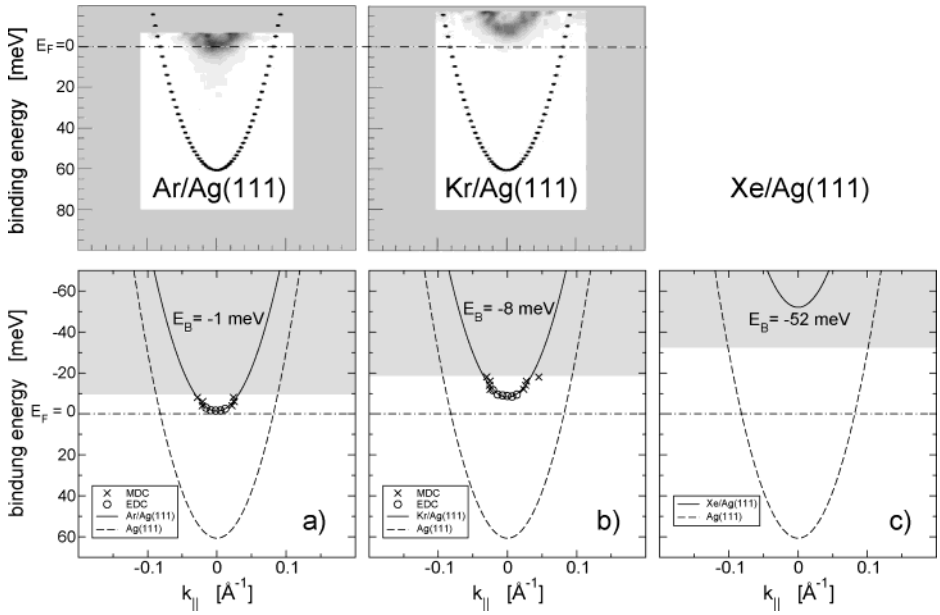

Figure 2. Photoemission data on the Ag(111) surface covered with 1 ML of different rare gases. The grayscale plot in the upper panel gives the photoemission intensity vs binding energy and parallel momentum along the $\bar{\Gamma}-\bar{K}$ direction after the normalization procedure described in the text. The dispersion of the clean Ag(111) surface is indicated as a dashed line. The temperatures during preparation and measurement were kept constant at $T = 22$ and 43 K for Ar and Kr, respectively. Lower panel: Analysis of the dispersions by a parabolic least-squares fit. The surface-state dispersion for Xe is out of the recoverable region of $5k_BT_{des}$ (gray area, T_{des} is the desorption temperature of the monolayer) and has been constructed from the results of STM measurements[34] for comparison ($T \approx 4$ K).

resolution, ΔE, is high enough (i.e., comparable to the thermal broadening $4k_BT$ or better), the noise is low, and the excitation is free from satellites.[36] The accessible energy range for photoemission can be extended to $5k_BT$ *above* E_F, just enough to recover the tail of the parabola for the data of the Ar and Kr monolayer systems. In the case of the Xe monolayer, the surface state is shifted to 52 meV above the Fermi level, i.e., far beyond the limit of the accessible energy range at 32 meV, taking the maximum experimental temperature defined by the desorption temperature of 75 K.[37] For comparison, we add for this system the results of an investigation by Hövel et al.,[34] who measured the surface state spectroscopically by STM, for which the energy

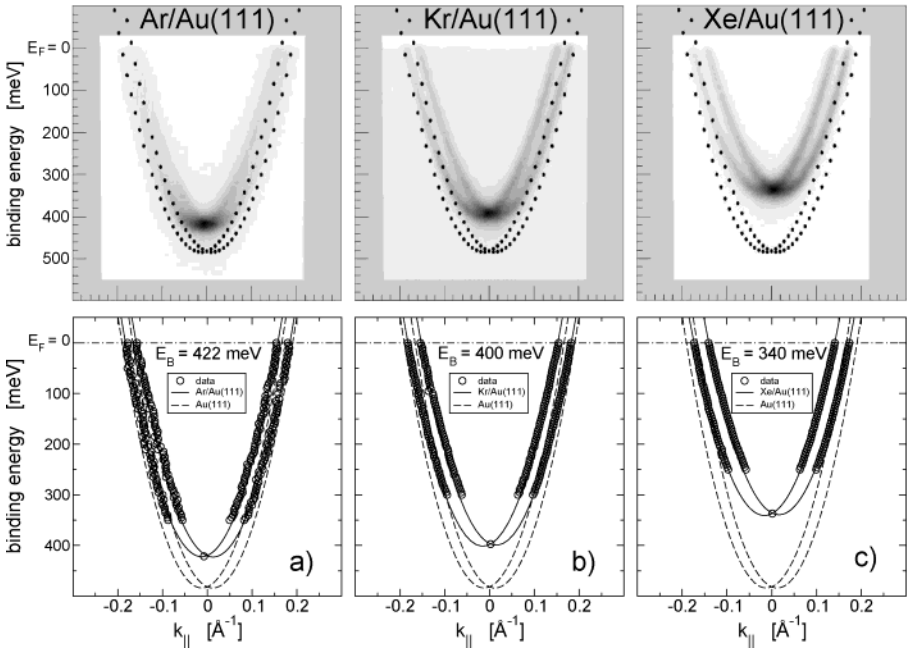

Figure 3. Photoemission data on the Au(111) surface covered with 1 ML of different rare gases. The grayscale plot in the upper panel gives the photoemission intensity vs binding energy and parallel momentum along the $\bar{\Gamma}-\bar{K}$ direction (dark is high intensity). The dispersion of the clean Au(111) surface is indicated as a dashed line. The temperatures during preparation and measurement were kept constant at $T = 25$, 40, and 50 K for Ar, Kr, and Xe, respectively. Lower panel: Analysis of the dispersions by a parabolic least-squares fit.

range is not restricted to the occupied states (see right panel of Figure 2). As in the case of Cu, there is—within the experimental accuracy—no change of the effective mass for all three rare gases. On the Ag(111) substrate, the rare-gas atoms form an incommensurate monolayer. As in the case of Ar and Kr on Cu(111), the superstructure is slightly expanded compared to 1 $\times$ 1.[38]

3.4. Rare Gases on Au(111). As described above, the Shockley state on Au(111) has a characteristic spin−orbit splitting that clearly can be observed in the photoemission data of the monolayer systems. Figure 3 gives the dispersion for the rare-gas-covered Au(111) surface, revealing the binding energy shift already known from the data on the Cu and Ag substrate. The monolayers have an incommensurate structure with an expansion factors of approximately 1.28, 1.35, and 1.38 for Ar, Kr, and Xe, respectively, determined from an analysis of the LEED spots. The LEED pattern (not shown here) indicates that the characteristic herringbone reconstruction of the Au(111) surface still exists below the rare-gas coverage.

As before, we analyzed the data by least-squares fit of the photoemission dispersion, but in this case with two identical parabolas shifted horizontally: $E_B = E_B^0 - \hbar^2(k_{||} \pm \Delta k_{||}/2)^2/2m^*$. Again, the effective mass remains constant for all investigated systems, whereas the spin−orbit splitting increases significantly for the adsorbate covered surfaces in comparison to the splitting of the Shockley state of the clean surface. In the case of the Xe monolayer, the splitting $\Delta k_{||}$ is approximately 30% larger than for the clean surface. In Figure 4, we relate the splittings with the binding energy, which decreases monotonically from clean Au(111) to Ar/Au(111) and from Kr/Au(111) to Xe/Au(111) (see below).

3.5. Discussion. Figure 5 gives a summary of the binding energies in Table 1 for the investigated systems. The rare gases are ordered on the *x* axis with increasing atomic number (i.e., decreasing nobleness) from left to right. The *y* axis gives the binding energy at the band minimum relative to the band minimum of the clean surface. For all substrates, the binding

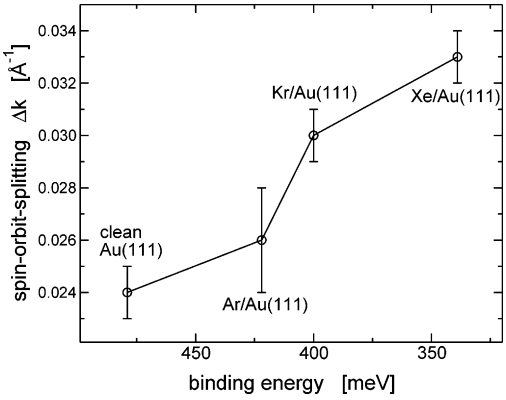

Figure 4. Spin-orbit spitting $\Delta k_{||}$ for the clean surface and the three investigated adsorbates Ar, Kr, and Xe on Au(111). The splitting is plotted vs the binding energy, which decreases with decreasing nobleness of the adsorbate.

energy shift increases from left to right. Furthermore, the shifts for the different substrates are nearly identical and—within the experimental accuracy—do depend only on the adsorbed rare gas. Only the value for Xe on Ag(111), determined by a spectroscopic measurement by STM,[34] differs clearly from the photoemission results on Xe/Cu(111) and Xe/Au(111). The reason for this difference might be partly the different experimental temperatures in the two experiments—the ARUPS measurements for Xe were performed at 50 K, whereas the STM spectra were measured at $T = 5$ K[6,31]—and also an influence of effects related to the experimental method, such as the Stark effect in STM, which can cause a current dependent shift of the Shockley-state binding energies, by up to 15 meV to higher binding energies for clean Ag(111), for example.[39]

The observed monotonic increase of the binding energy is not as obvious as it appears at first glance. In the case of Cu(111), the least-noble rare gas, i.e., Xe, has a different structural order than the other investigated gases. Whereas Kr and Ar form an incommensurate overlayer, Xe adsorbs on Cu(111) as a $\sqrt{3}$

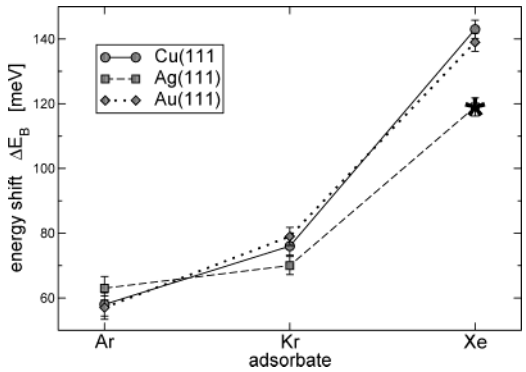

Figure 5. Relative shift of the Shockley state in comparison to the clean substrate surface at $T = 30$ K. The systems were measured at different temperatures (see captions of Figures 1−3), slightly influencing the measured binding energies. The data point for Xe on Ag(111) was taken from an STM measurement by Hövel et al. at $T = 5$ K.[34]

$\times \sqrt{3}R30°$ superstructure (see Figure 6). In this case, all Xe atoms adsorb on identical on-top sites,[35] whereas for the incommensurate phase the adsorption site varies for different rare-gas atoms. Although different sites might differ significantly in the local adsorption energy, the effect averages out in the influence on the binding energy shift of the Shockley state.

As already demonstrated in Figure 4, the same continuous behavior can be observed for the spin−orbit splitting (SOS) of the Shockley state on Au(111). This indicates that the mechanisms responsible for SOS are related to the electrostatic potentials at the surface that are also responsible for the binding energy shift. However, no obvious and simple explanation has yet been provided, although slab-layer calculations by density functional theory methods are able to describe the change of both binding energy and SOS.[40] The work function change, which is typically on the order of 0.5 eV,[41] plays only a minor role in this context because its contribution to the gradient of the potential is not sufficient to explain the observed magnitude of the SOS.[27] Another parameter is the increased surface corrugation,[29] but a clear correspondence with the observed changes in the SOS is not discernible. Photoemission measurements on thin epitaxial Ag films on Au(111) show a *decrease* of the SOS[42,43] with increasing film thickness. In this case, however, there is a gradual change from the properties of Au(111) to those of the Ag(111) surface, on which the SOS of the Shockley state is 1 order of magnitude smaller than for clean Au(111).[28]

The binding energy shift is usually explained by the picture of the Pauli repulsion, where the repulsive short-range interaction is a consequence of the overlapping wave functions of the closed shell of the rare-gas atoms with the wave function of the substrate, exponentially decaying outside the crystal. In this weak-interaction picture,[14−17] the orthogonality of the metal states to the nearly unperturbed atomic wave functions induces an oscillation of the metal wave functions in the region of the rare-gas core, and the charge from the evanescent tail is driven back into the substrate. As a consequence, the binding energies of the Bloch electrons—including the Shockley-state electrons—are shifted toward the Fermi level, so that the net interaction potential can be described by the integral over the energy shifts of all involved states plus the attractive van der Waals potential. Because the Shockley states are spatially confined to the surface region, they show the strongest influence of this effect. The electrons from the surface density of states, which is shifted through the Fermi level, are transferred into the Bloch states of the bulk.

Possibly, the spatial modification of the Shockley-state wave function by the Pauli repulsion results in a shift of the electron density to regions where the net gradient of the potential is larger. Because the Rashba term α_R, giving the SOS of the Shockley state (see, e.g., ref 27), is proportional to the gradient of the potential, this would result in an increase of the observed splitting with an increasing perturbation of the Shockley-state wave function. However, for a quantitative understanding of the observed SOS increase of up to 30% in the case of Xe, further theoretical studies are necessary.

3.6. Commensurate Phase and Back-Folding: Xe on Cu(111). Finally, we briefly discuss the $\sqrt{3} \times \sqrt{3}R30°$ superstructure of the Xe monolayer on Cu(111). The reduced hexagonal surface Brillouin zone (SBZ) of the adsorbate system appears as additional spots in the LEED pattern (panel b in Figure 6). In correspondence with the new SBZ, the Shockley

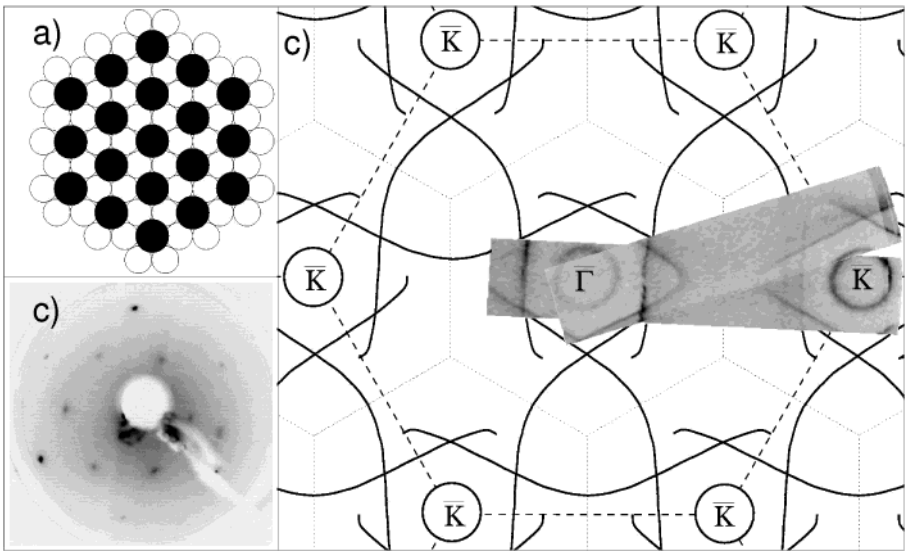

Figure 6. Superstructure and Fermi surface map (FSM) of 1 ML Xe on Cu(111). The upper panel on the left (a) shows the geometric structure of the Xe adatoms (black) on the substrate surface (white). This $\sqrt{3} \times \sqrt{3}R30°$ on-top superstructure can be observed as additional spots in the form of the inner hexagon in the LEED pattern given in panel b ($E_0 = 120$ eV). Panel c displays the measured FSM as a grayscale plot in addition to the back-folded Fermi surfaces from LDA calculations.[44] $\bar{K}$ and $\bar{\Gamma}$ mark the high-symmetry points of the surface Brillouin zone (SBZ) of the clean Cu(111) surface.

state can be observed at the back-folded $\bar{\Gamma}$ points, i.e., at the $\bar{K}$ points of the Cu(111) SBZ. In photoemission, such a back-folding of the surface states has been observed for other systems, e.g., Xe on HOPG (highly oriented pyrolytic graphite),[45] Cu_3-Au,[46] the "herringbone" reconstructed Au(111) surface,[32] and Si(111) $\sqrt{21} \times \sqrt{21}$-(Ag,Au).[47] Panel c of Figure 6 shows the Fermi surface map (FSM) of the Xe-covered Cu(111) surface. The FSM gives the photoemission intensity vs $\mathbf{k}_{||} = (k_x, k_y)$ as a grayscale plot over two overlapping measured stripes (high intensity appears dark). The vertical width of the stripes is determined by the parallel detected angular range, the length represents a tilt angle range from $-64°$ to $+16.5°$ with a step width of 0.5°. Note that the circular Fermi surface of the back-folded Shockley state centered at $\bar{K}$ appears even more intense than that of the "original" at $\bar{\Gamma}$. Around the two measured Shockley states at $\bar{\Gamma}$ and $\bar{K}$, there appears an additional intensity forming nearly straight and narrow lines. The origin of this additional intensity becomes clear when we compare the FSM with the back-folded Fermi surface map of the Cu(111) surface. As known from the He I measurements on Cu(111) published in the literature (see ref 48 and references therein), the cut through the belly-neck-shaped bulk Fermi surface of Cu forms an intensity distribution with a 3-fold rotational symmetry, with the necks appearing at the $\bar{M}'$ points of the SBZ. The FSM of the Xe-covered Cu(111) surface is constructed by back-folding this bulk FSM (plus the circular Shockley-state FSMs centered at $\bar{\Gamma}$) at the new zone boundaries of the reduced SBZ. The result, given as solid lines in Figure 6, nicely coincides with the observed intensity distribution. The overlapping bulk bands form a hexagon around the circular Fermi surfaces of the Shockley state at normal emission ($\bar{\Gamma}$ point) and the former $\bar{K}$ points. Obviously, although the coupling between adsorbate and substrate is weak, the Xe adlayer results in a perfect back-folding of the angle-resolved photoemission intensity of the Cu(111) surface. Although the back-folding indicates that the Xe monolayer is well-ordered, there must exist additional defects in comparison to the clean surfaces: the *L* gap, which could be observed as a minimum intensity ring around the Shockley-state Fermi surface of the clean surfaces,[23] cannot be resolved here. However, the influence of this additional defect scattering on the line width of the Shockley state is small.[24]

4. Conclusions

We have presented a systematic photoemission study on Shockley states on noble-metal (111) surfaces covered with a rare-gas monolayer. Although the interaction between adsorbate and substrate is weak, the monolayer causes a significant binding energy shift and—in the case of Au(111)—an increase of the spin−orbit splitting of the Shockley state as compared to that of the clean surface. The observed effects can be qualitatively understood by the influence of the Pauli repulsion between the closed-shell atoms and the Shockley-state wave function out of the crystal. The high sensitivity to surface modifications makes the Shockley states an important tool for understanding the physics at interfaces, in particular, the interaction between adsorbates and solids. We hope that this work stimulates the investigation of the Shockley states in first-principles calculations on adsorbate and thin-film systems.

Acknowledgment. This work was supported by the Deutsche Forschungsgemeinschaft (Grants Hu 149-19 and SFB 277). We thank Dr. Valeri G. Grigoryan and Prof. Michael Springborg, Universität des Saarlandes, for very helpful discussions.

References and Notes

(1) Shockley, W. On the surface states associated with a periodic potential. *Phys. Rev.* **1939**, *56*, 317−323.

(2) Gartland, P. O.; Slagsvold, B. J. Transition conserving parallel momentum in photoemission from the (111) face of copper. *Phys. Rev. B* **1975**, *12* (10), 4047−4058.

(3) Davison, S. G.; Steslicka, M. *Basic Theory of Surface States*; Oxford University Press: Oxford, U.K., 1992.

(4) Heimann, P.; Neddermeyer, H.; Roloff, H. F. Ultraviolet photoemission from intrinsic surface states of the noble metals. *J. Phys.: Condens. Matter* **1977**, *10*, L17−L21.

(5) Kevan, S. D.; Gaylord, R. H. High-resolution photoemission study of the electronic structure of the noble-metal (111) surfaces. *Phys. Rev. B* **1987**, *36* (11), 5809−5818.

(6) Paniago, R.; Matzdorf, R.; Meister, G.; Goldmann, A. Temperature dependence of Shockley-type surface energy bands on Cu(111), Ag(111) and Au(111). *Surf. Sci.* **1995**, *336*, 113−122.

(7) Li, J.; Schneider, W.-D.; Berndt, R.; Bryant, O. R.; Crampin, S. Surface state lifetime measured by scanning tunneling spectroscopy. *Phys. Rev. Lett.* **1998**, *81* (20), 4464−4467.

(8) Bürgi, L.; Petersen, L.; Brune, H.; Kern, K. Noble metal surface states: Deviations from parabolic dispersion. *Surf. Sci.* **2000**, *447*, L157−L161.

(9) Kliewer, J.; Berndt, R.; Chulkov, E. V.; Silkin, V. M.; Echenique, P. M.; Crampin, S. Dimensionality effects in the lifetime of surface states. *Science* **2000**, *288*, 1399−1402.

(10) Echenique, P. M.; Pitarke, J. M.; Chulkov, E. V.; Rubio, A. Theory of inelastic lifetimes of low-energy electrons in metals. *Chem. Phys.* **2000**, *251*, 1−35.

(11) Eiguren, A.; Hellsing, B.; Reinert, F.; Nicolay, G.; Chulkov, E. V.; Silkin, V. M.; Hüfner, S.; Echenique, P. M. Role of bulk and surface phonons in the decay of metal surface states. *Phys. Rev. Lett.* **2002**, *88* (6), 066805.

(12) Hellsing, B.; Eiguren, A.; Reinert, F.; Nicolay, G.; Chulkov, E. V.; Silkin, V. M.; Hüfner, S.; Echenique, P. M. Lifetime of holes and electrons at metal surfaces; electron−phonon coupling. *J. Electron Spectrosc. Relat. Phenom.* **2003**, *129*, 97−104.

(13) Bertel, E., Donath, M. Eds. *Electronic Surface and Interface States on Metallic Systems*; World Scientific: Singapore, 1994.

(14) Bruch, L. W.; Cole, M. W.; Zaremba, E. *Physical Adsorption: Forces and Phenomena*; Oxford University Press: Oxford, U.K., 1997.

(15) Bertel, E.; Memmel, N. Promotors, poisons and surfactants: Electronic effects of surface doping on metals. *Appl. Phys. A* **1996**, *63*, 523−531.

(16) Zaremba, E.; Kohn, W. Theory of helium adsorption on simple and noble-metal surfaces. *Phys. Rev. B* **1977**, *15* (4), 1769−1781.

(17) Harris, J.; Liebsch, A. Interaction of helium with a metal surface. *J. Phys. C: Solid State Phys.* **1982**, *15*, 2275−2291.

(18) Piot, L. Untersuchungen zur elektronischen Struktur dünner organischer Filme. Diplomarbeit, Universität des Saarlandes, Saarbrücken, Germany, 2003.

(19) Nicolay, G.; Reinert, F.; Schmidt, S.; Ehm, D.; Steiner, P.; Hüfner, S. Natural line width of the Ag(111) L-gap surface state as determined by photoemission spectroscopy. *Phys. Rev. B* **2000**, *62* (3), 1631−1634.

(20) Reinert, F.; Nicolay, G.; Eltner, B.; Ehm, D.; Schmidt, S.; Hüfner, S.; Probst, U.; Bucher, E. Observation of a BCS spectral function in a conventional superconductor by photoelectron spectroscopies. *Phys. Rev. Lett.* **2000**, *85* (18), 3930−3933.

(21) Reinert, F.; Eltner, B.; Nicolay, G.; Ehm, D.; Schmidt, S.; Hüfner, S. Electron−phonon coupling and its evidence in the photoemission spectra of lead. *Phys. Rev. Lett.* **2003**, *91* (18), 186406.

(22) Nicolay, G.; Reinert, F.; Hüfner, S.; Blaha, P. Spin−orbit splitting of the *L*-gap surface state on Au(111) and Ag(111). *Phys. Rev. B* **2002**, *65*, 033407.

(23) Reinert, F.; Nicolay, G.; Schmidt, S.; Ehm, D.; Hüfner, S. Direct measurements of the *L*-gap surface states on the (111) face of noble metals by photoelectron spectroscopy. *Phys. Rev. B* **2001**, *63*, 115415.

(24) Forster, F.; Nicolay, G.; Reinert, F.; Ehm, D.; Schmidt, S.; Hüfner, S. Interface and surface states on adsorbate covered noble metal surfaces. *Surf. Sci.* **2003**, *532*−*535*, 160−165.

(25) Nicolay, G.; Reinert, F.; Forster, F.; Ehm, D.; Schmidt, S.; Eltner, B.; Hüfner, S. About the stability of noble metal surface states during VUV experiments. *Surf. Sci.* **2003**, *543*, 47−56.

(26) LaShell, S.; McDougall, B. A.; Jensen, E. Spin splitting of an Au(111) surface state band observed with angle resolved photoelectron spectroscopy. *Phys. Rev. Lett.* **1996**, *77* (16), 3419−3422.

(27) Petersen, L.; Hedegård, P. A simple tight-binding model of spin−orbit splitting of sp-derived surface states. *Surf. Sci.* **2000**, *459*, 49−56.

(28) Reinert, F. Spin−orbit interaction in the photoemission spectra of noble metal surface states. *J. Phys.: Condens. Matter* **2003**, *15*, S693−S705.

(29) Henk, J.; Ernst, A.; Bruno, P. Spin polarization of the *L*-gap surface state on Au(111). *Phys. Rev. B* **2003**, *68*, 165416.

(30) Muntwiler, M.; Hoesch, M.; Petrov, V. N.; Hengsberger, M.; Patthey, L.; Shi, M.; Falub, M.; Greber, T.; Osterwalder, J. Spin- and angle-resolved photoemission spectroscopy study of the Au(111) Shockley surface state, manuscript to be published.

(31) Nicolay, G. Untersuchungen zur elektronischen Struktur in situ-präparierter Edelmetalloberflächen. Ph.D. Thesis, Universität des Saarlandes, Saarbrücken, Germany, Oct 2002.

(32) Reinert, F.; Nicolay, G. Influence of the herringbone reconstruction on the surface electronic structure of Au(111). *Apl. Phys. A* **2004**, *78*, 817−821.

(33) Reinert, F.; Eltner, B.; Nicolay, G.; Forster, F.; Schmidt, S.; Hüfner, S. The electron−phonon selfenergy of metallic systems determined by angular resolved high-resolution photoemission. *Physica B*, in press.

(34) Hövel, H.; Grimm, B.; Reihl, B. Modification of the Shockley-type surface state on Ag(111) by an adsorbed xenon layer. *Surf. Sci.* **2001**, *477*, 43−49.

(35) Da Silva, J. L. F.; Stampfl, C.; Scheffler, M. Adsorption of Xe on metal surfaces: New insights from first-principles calculations. *Phys. Rev. Lett.* **2003**, *90* (6), 66104.

(36) Greber, T.; Kreutz, T. J.; Osterwalder, J. Photoemission above the Fermi level: The top of the minority *d* band in nickel. *Phys. Rev. Lett.* **1997**, *79* (22), 4465−4468.

(37) Gibson, K. D.; Sibener, S. J. Inelastic helium scattering studies of the vibrational spectroscopy and dynamics of ordered Ar, Kr, and Xe multilayers physisorbed on Ag(111). *J. Chem. Phys.* **1988**, *88* (12), 7893−7910.

(38) Unguris, J.; Bruch, L. W.; Moog, E. R.; Webb, M. W. Ar and Kr adsorption on Ag(111). *Surf. Sci.* **1981**, *109*, 522−556.

(39) Limot, L.; Maroutian, T.; Johansson, P.; Berndt, R. Surface-state Stark shift in a scanning tunneling microscope. *Phys. Rev. Lett.* **2003**, *91* (19), 196801.

(40) Grigoryan, V. G.; Springborg, M. Wien2k calculations of the Shockley-state spin−orbit splitting on rare-gas covered noble metal surfaces, manuscript to be published.

(41) Wolf, M.; Knoesel, E.; Hertel, T. Ulrafast dynamics of electrons in image-potential states on clean and Xe-covered Cu(111). *Phys. Rev. B* **1996**, *54* (8), R5295−R5298.

(42) Cercellier, H.; Fagot-Revurat, Y.; Kierren, B.; Malterre, D.; Reinert, F. Shockley state in epitaxial Ag films on Au(111). *Surf. Sci.*, in press, published online.

(43) Cercellier, H.; Fagot-Revurat, Y.; Kierren, B.; Reinert, F.; D. Popović, Malterre, D.; Spin−orbit splitting of the Shockley state in the Ag/Au(111) interface. *Phys. Rev. B*, accepted.

(44) Aebi, P.; Fasel, R.; Naumovic, D.; Hayoz, J.; Pillo, Th.; Bovet, M.; Agostino, R. G.; Patthey, L.; Schlapbach, L.; Gil, F. G.; Berger, H.; Krentz, T. J.; Osterwalder, J. *Surf. Sci.* **1998**, *402−404*, 614.

(45) Patthey, F.; Schaffner, M.-H.; Schneider, W.-D.; Delley, B. Brillouin zone-folding and Fano resonances in commensurate rare gas monolayers observed in photoemission. *Surf. Sci.* **2000**, *454−456*, 483−488.

(46) Courths, R.; Lau, M.; Scheunemann, T.; Gollisch, H.; Feder, R. From the Shockley surface state on Cu(111) to sp-like surface resonances on Cu_3Au. *Phys. Rev. B* **2001**, *63*, 195110.

(47) Crain, J. N.; Altmann, N. K.; Bromberger, C.; Himpsel, F. J. Fermi surfaces of surface states on Si(111)−Ag, Au. *Phys. Rev. B* **2002**, *66*, 205302.

(48) Hüfner, S. *Photoelectron Spectroscopy. Principles and Applications*, 3rd ed.; Springer-Verlag: New York, 2003.